Interaction of phosphodiesterase 3A with brefeldin A-inhibited guanine nucleotide-exchange proteins BIG1 and BIG2 and effect on ARF1 activity

Ermanno Puxeddu, Marina Uhart, Chun-Chun Li, Faiyaz Ahmad, Gustavo Pacheco-Rodriguez, Vincent C. Manganiello, Joel Moss, and Martha Vaughan[1]

Translational Medicine Branch, National Heart, Lung, and Blood Institute, National Institutes of Health, Bethesda, MD 20892

Contributed by Martha Vaughan, February 11, 2009 (sent for review September 22, 2008)

ADP-ribosylation factors (ARFs) have crucial roles in vesicular trafficking. Brefeldin A-inhibited guanine nucleotide-exchange proteins (BIG)1 and BIG2 catalyze the activation of class I ARFs by accelerating replacement of bound GDP with GTP. Several additional and differing actions of BIG1 and BIG2 have been described. These include the presence in BIG2 of 3 A kinase-anchoring protein (AKAP) domains, one of which is identical in BIG1. Proteins that contain AKAP sequences act as scaffolds for the assembly of PKA with other enzymes, substrates, and regulators in complexes that constitute molecular machines for the reception, transduction, and integration of signals from cAMP or other sources, which are initiated, propagated, and transmitted by chemical, electrical, or mechanical means. Specific depletion of HeLa cell PDE3A with small interfering RNA significantly decreased membrane-associated BIG1 and BIG2, which by confocal immunofluorescence microscopy were widely dispersed from an initial perinuclear Golgi concentration. Concurrently, activated ARF1-GTP was significantly decreased. Selective inhibition of PDE3A by 1-h incubation of cells with cilostamide similarly decreased membrane-associated BIG1. We suggest that decreasing PDE3A allowed cAMP to accumulate in microdomains where its enzymatic activity limited cAMP concentration. There, cAMP-activated PKA phosphorylated BIG1 and BIG2 (AKAPs for assembly of PKA, PDE3A, and other molecules), which decreased their GEP activity and thereby amounts of activated ARF1-GTP. Thus, PDE3A in these BIG1 and BIG2 AKAP complexes may contribute to the regulation of ARF function via limitation of cAMP effects with spatial and temporal specificity.

ADP-ribosylation factors (ARFs) are members of the Ras superfamily of ≈20-kDa GTPases that have diverse roles in intracellular vesicular trafficking. ARF binding to donor membranes initiates the formation of vesicles for regulated translocation of protein and lipid molecules among eukaryotic cell organelles. This action requires cycling between inactive, largely cytosolic ARF-GDP, and GTP-bound active, membrane-associated forms (1–3). Conversion of ARF-GDP to ARF-GTP is catalyzed by guanine nucleotide-exchange proteins (GEPs), which accelerate the release of bound GDP to permit GTP binding. All known GEPs, although they differ in molecular size and structure, share a highly conserved central sequence of ≈200 aa, the Sec7 domain, that is responsible for this function (4–5). Sensitivity of GEP activity to inhibition by brefeldin A (BFA), a fungal fatty acid metabolite that blocks protein secretion (6), distinguishes 2 major groups. BFA-inhibited GEP (BIG)1 (≈200 kDa) and BIG2 (≈190 kDa) were first purified together in >670-kDa multiprotein complexes from bovine brain cytosol, based on assays of BFA-inhibited ARF activation (7). The molecules are 74% identical in overall amino acid sequences, with 90% identity in Sec7 and other domains (8). Systematic yeast 2-hybrid screening was used to identify their potentially functional interactions with other proteins.

The N-terminal BIG1 sequence (1-331) interacted with FK506-binding protein 13 (9), and the C-terminal region of the molecule with myosin IX-b (10), as well as with kinesin KIF21A (11). Two-hybrid interaction of the BIG2 N-terminal region with exocyst subunit Exo70 was confirmed by coimmunoprecipitation (co-IP) of the in vitro-translated proteins; microscopically, the endogenous proteins appeared together along microtubules (12); 3 A kinase-anchoring protein (AKAP) sequences in the N-terminal region of BIG2, one of which is identical in BIG1, were identified in yeast 2-hybrid experiments with 4 different A kinase R subunits and multiple peptide sequences representing positions 1 to 643 of BIG2 (13). Consistent with the presence of AKAP sequences for each of the 4 R subunits in BIG1 and BIG2, both proteins were coimmunoprecipitated from HepG2 cell cytosol with antibodies against RI or RII, although direct interaction of the molecules was not established (13). PKA-catalyzed phosphorylation of endogenous BIG1 in HepG2 cells resulted in its rapid nuclear accumulation (14). Differences between mechanisms, and perhaps functions, of BIG1 accumulation in nuclei after cAMP elevation and after serum deprivation remain to be determined. In vitro experiments with BIG1 and BIG2 immunoprecipitated from HepG2 cells that had been selectively depleted, respectively, of BIG2 or BIG1, showed that phosphorylation catalyzed by recombinant PKA catalytic unit decreased GEP activity with recombinant ARF1-GST; activity was restored by incubation with recombinant protein phosphatase PP1γ, which dephosphorylated BIG1 and BIG2 (15).

Because of demonstrated AKAP characteristics of these GEP molecules with their functions in ARF activation and vesicular trafficking at different intracellular sites, we expected to find a cAMP phosphodiesterase (PDE) component that would terminate the cAMP signal to parallel PP1γ reversal of PKA phosphorylation (15–17). We report here the co-IP of PDE3A with BIG1 or BIG2 from HeLa cell cytosol, which contains also isoform PDE3B. Selective inhibition of PDE3 with cilostamide or specific depletion of PDE3A with siRNA significantly decreased membrane-associated BIG1 and BIG2; microscopically, immunofluorescence of endogenous BIG1 and BIG2 was widely dispersed from the initial Golgi region concentrations. Thus, PDE3A was another component of these BIG1 and BIG2 AKAP complexes that can contribute to the regulation of ARF function with specificity of location as well as of timing.

Results

Association of PDE Activity with BIG1 and BIG2 Complexes. To demonstrate association of BIG1 and BIG2 with a PDE, proteins precipitated from HeLa cell cytosol with antibodies against

Author contributions: E.P., V.C.M., J.M., and M.V. designed research; E.P., M.U., C.-C.L., F.A., and G.P.-R. performed research; E.P., V.C.M., J.M., and M.V. analyzed data; and E.P., V.C.M., J.M., and M.V. wrote the paper.

The authors declare no conflict of interest.

Freely available online through the PNAS open access option.

[1]To whom correspondence should be addressed. E-mail: vaughanm@mail.nih.gov.

This article contains supporting information online at www.pnas.org/cgi/content/full/0901558106/DCSupplemental.

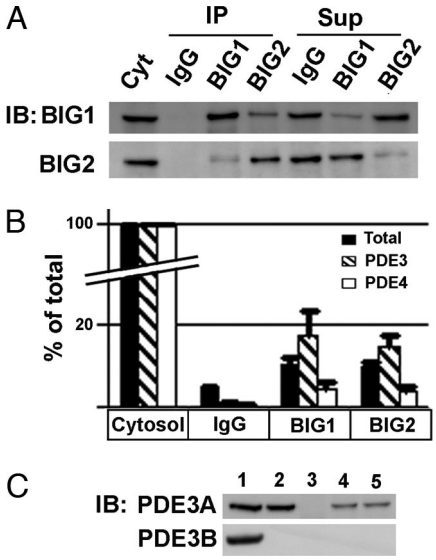

Fig. 1. Co-IP of PDE with BIG1 and BIG2. (*A*) After IP of cytosol proteins (500 μL, 500 μg) with BIG1 and BIG2 antibodies or control rabbit IgG, bead-bound proteins were eluted in 120 μL of gel-loading buffer. Samples of cytosol and supernatant (1/25), or eluted proteins (1/6) from IP were separated by SDS/PAGE for IB with antibodies against BIG1 and BIG2. (*B*) Total, PDE3 and PDE4 activities (pmol/min) were assayed by using duplicate samples from 1/2 of each IP. Activities in each experiment were expressed as percentage of that in cytosol = 100%. Data are reported as means ± SE of values from 3 experiments. (*C*) Samples of lysate (20-μg protein) (lane 1), cytosol (lane 2), and immunoprecipitated proteins (lane 3, IgG; lane 4, BIG1; and lane 5 BIG2) were separated as in Fig. 1*A*, and reacted (IB) with antibodies against PDE3A or PDE3B. Data were similar in 2 more experiments.

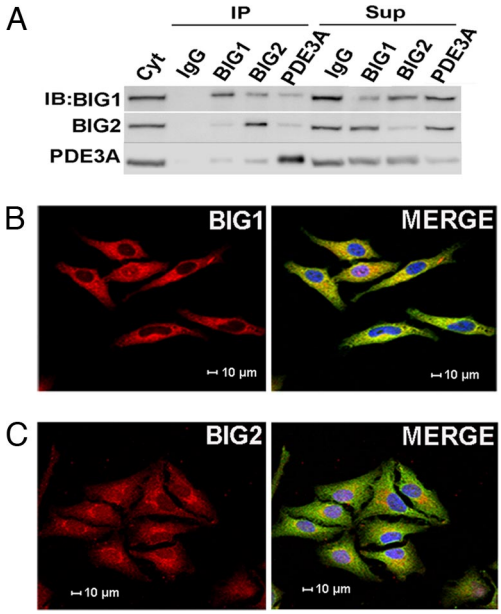

Fig. 2. Intracellular localization of PDE3A, BIG1, and BIG2. (*A*) After IP of cytosol as in Fig. 1*A* with control IgG or antibodies against BIG1, BIG2, or PDE3A, samples (1/12) of precipitated proteins (IP), and of cytosol or supernatant (1/25) were subjected to Western blotting (IB) with indicated antibodies. Data were similar in 3 experiments. (*B* and *C*) Confocal laser-scanning microscopy of cells reacted with antibodies against (*B*) BIG1 (red), or (*C*) BIG2 (red), and PDE3A (green). Merge represents BIG1 or BIG2 with PDE3A. Data were similar in 2 more experiments.

BIG1 or BIG2 or normal IgG were assayed for PDE activity. IP of >90% of BIG1 yielded also ≈15% of BIG2. Similarly, BIG2 antibodies precipitated ≈90% of BIG2 and 15% of BIG1, whereas neither protein was detected after IgG IP (Fig. 1*A*). Type3 and type4 PDE activities (Fig. 1*B*) were defined as those inhibited, respectively, by 1 μM cilostamide and 5 μM rolipram (17). Identity of the PDE(s) responsible for the additional activity included in "total" was not investigated. Activity precipitated with normal IgG was much less than that with antibodies against BIG1 or BIG2, and PDE3 or PDE4 activity was not detected.

PDE3 activity precipitated with BIG1 antibodies was 17.5 ± 5% of that in cytosol, and PDE4 was 4.2 ± 2% of cytosol activity (Fig. 1*B*). BIG2 IP yielded 14.7 ± 2.6% of PDE3 activity, and 4.0 ± 1.4% of PDE4 (Fig. 1*B*). Western blotting confirmed IP of PDE3A protein with BIG1 and BIG2 antibodies. Although both immunoreactive PDE3A and PDE3B were present in HeLa cell lysates, only PDE3A was detected in cytosol, and was precipitated with BIG1 and BIG2 antibodies (Fig. 1*C*).

IP of BIG1 and BIG2 with PDE3A and Partial Intracellular Colocalization. Ninety percent of endogenous BIG1, BIG2, or PDE3A was precipitated from cytosol with the respective antibodies along with 10–15% of the other 2 proteins, none of which was precipitated with control IgG (Fig. 2*A*). On confocal immunofluorescence microscopy, overall distributions of endogenous BIG1 and BIG2 were clearly different, although both appeared in punctate collections throughout the cytoplasm, and concentrated in the perinuclear region, consistent with Golgi structures. PDE3A was also concentrated in the perinuclear region where it seemed to coincide with BIG1 and BIG2. However, more diffusely distributed PDE3A was not evidently colocalized with BIG1 or BIG2 (Fig. 2 *B* and *C*).

BIG1, BIG2, PDE3A, and RI α in Cytosolic Complexes. After Superose 6 gel filtration of cytosol, BIG1 and BIG2 were found in fractions with molecules of >670 kDa, consistent with past findings (18). PDE3A was recovered in 2 peaks, the first of >3,000 kDa, and the second largely coincident with BIG1 and BIG2; >90% of PKA RIα subunit was in fractions of ≈200 kDa, but it was also present in fractions 26–30 with BIG1, BIG2, and PDE 3A; RII β was detected exclusively with molecules of smaller size (Fig. 3*A*). PDE3 activity (Fig. 3*B*) was demonstrated in fractions forming 2 immunoreactive PDE3A protein peaks in Fig. 3*A*. IP of PDE3A from pooled fractions 15–19 and 26–30, which contained also BIG1, BIG2, and RI α, was consistent with the presence of BIG1, BIG2, PDE3A, and PKA RIα together in multiprotein complexes of >670 kDa (Fig. 3*C*).

Effect of PDE3A Inhibition on Intracellular Distribution of BIG1. In vitro assay of PDE3 and PDE4 activities depends on their selective inhibition by cilostamide and rolipram, respectively. After 1-h incubation of cells with cilostamide, PDE3 activity was 81% lower than that in untreated cells, and PDE4 was only 9% lower. Conversely, rolipram treatment decreased cell PDE4 and PDE3 activities by 91 and 9%, respectively (Fig. 4*A*). Recovery of BIG1 in membrane fractions from cilostamide-treated cells was significantly lower, and that in cytosol significantly higher than from untreated cells; however, rolipram inhibition of PDE4 had no effect on BIG1 distribution (Fig. 4*B*).

Effect of PDE3A Depletion on Intracellular Distribution of BIG1 and BIG2. Treatment with PDE3A-specific siRNA for 48 h decreased the endogenous protein by 90% (Fig. 5 *A* and *B*), and decreased BIG1 and BIG2 in membrane fractions by 40%, with no effects of other treatments (Fig. 5*B*). Microscopically, BIG1 and GM130, a *cis*-Golgi marker, were concentrated together at perinuclear, presumably Golgi, membranes in untreated cells or in those treated with control nontargeting siRNA (Fig. 5*C*).

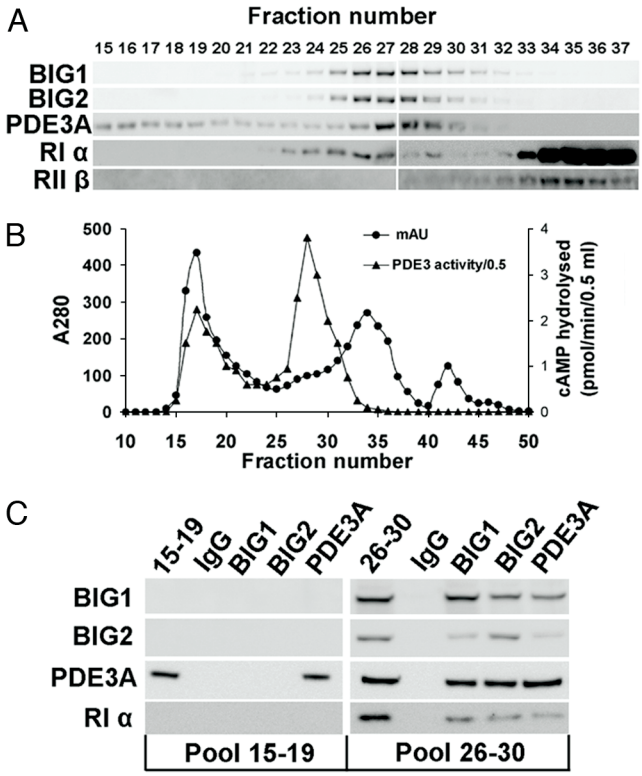

Fig. 3. Separation of cytosolic PDE 3A, BIG1, BIG2, and PKA regulatory subunits by gel filtration. (*A*) Samples (20 μL) of indicated cytosol fractions (0.5 mL) separated on Superose 6 were subjected to Western blotting with the indicated antibodies. (*B*) Protein content (AU 280 nm, ·) and PDE3 activity (pmol/min, ▲) of fractions in *A*. (*C*) After IP of pooled fractions 15–19 and 26–30 (240 μL each) with antibodies against BIG1, BIG2, or PDE 3A or control IgG, samples (1/12) of each pool (15–19 or 26–30), and precipitated proteins (1/12) were analyzed by Western blotting with indicated antibodies.

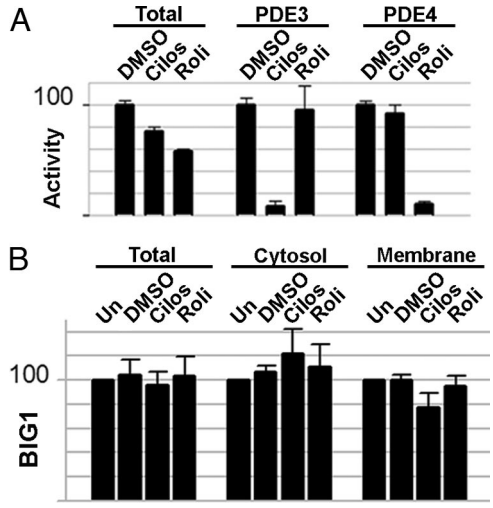

Fig. 4. Effect of PDE3 and PDE4 inhibition on BIG1 distribution in cells. (*A*) Cells were incubated 1 h with vehicle (DMSO), 14 μM cilostamide (cilos), or 30 μM rolipram before preparation of postnuclear supernatant fractions and assay of the indicated PDE activities. Data are means ± SE of triplicate assays with activities expressed relative to that of activity of the same PDE in cells incubated with vehicle alone = 100. (*B*) Cells were untreated or incubated 1 h with DMSO, cilostamide, or rolipram as in *A*. Samples of postnuclear supernatant (total, 1/25), cytostol (1/25), and membranes (1/6) were analyzed by Western blotting for BIG1. Data are means ± SD, of values from 3 experiments quantified by densitometry and expressed relative to that of untreated cells in the same experiment = 100. BIG1 levels in cytosol from cilostamide-treated cells were significantly higher, and in membranes lower than those in untreated cells ($P \leq 0.05$).

Although BIG2 was similarly concentrated in the perinuclear region, its coincidence with GM130 was much less clear, consonant with its demonstrated action in TGN trafficking (19, 20). After depletion of PDE3A, BIG1 and BIG2 were dispersed throughout the cytoplasm (Fig. 5*C*), consistent with results of subcellular fractionation (Fig. 5 *A* and *B*).

These observations were replicated with 2 more PDE3A-specific siRNAs, which were used also for data in Figs. S1–S3.

Effect of 8-Br-cAMP on Association of BIG, BIG2, and PDE3A. IP of BIG1 or BIG2 from cytosol coprecipitated PDE3A (Fig. 1). Brief incubation of cytosol with 8-Br-cAMP did not alter total proteins, but increased amounts of PDE3A immunoprecipitated with BIG1 or BIG2 (Fig. 6*A*). Although percentages of coprecipitated PDE4 or total PDE activities were not affected by 8-Br-cAMP, percentages of PDE3A activity immunoprecipitated with BIG1 and BIG2 were significantly increased (Fig. 6*B*). However, incubation of cells with 8-Br-cAMP resulted in nuclear accumulation of BIG1, (Fig. S4) as had been reported in HepG2 cells (14). This effect clearly did not resemble the wide cytoplasmic dispersion of BIG1 (and BIG2) seen after PDE3A depletion (Fig. 5*C*).

Effect of PDE3A Depletion on Amount of Active ARF1-GTP. PKA-catalyzed phosphorylation of BIG1 and BIG2 in vitro decreased their GEP activities (15). Depletion of PDE3A was expected to result in elevation of cAMP content of domains in which AKAP-tethered PDE3A regulates cAMP concentration. We used GST-GGA3 pull-down assays (21) to compare amounts of active endogenous ARF1, ARF5, and ARF6 in untreated cells and in cells treated with nontargeting or specific PDE3A siRNA or vehicle alone (Fig. 7). Depletion of PDE3A did not alter amounts of BIG1, BIG2, actin, or the 3 ARFs. It likewise had no effect on amounts of ARF5-GTP or ARF6-GTP, which are believed not to be activated by BIG1 and BIG2. However, active ARF1-GTP bound to GST-GGA3 was decreased 44 ± 5% ($n = 3$; $P < 0.05$) from that in untreated cells (Fig. 7*B*), consistent with the inhibitory effect of phosphorylation of BIG1 and BIG2 on ARF1 activation that had been demonstrated in vitro (15). ARF1-GTP was decreased even more by 2 other PDE3A siRNAs that decreased PDE3A content by >90% (Fig. S3).

Discussion

The cAMP produced by adenylyl cyclase has potentially multiple diverse actions that result from its interaction with R subunits of PKA and/or other molecules at numerous intracellular sites. Many of the known cAMP effects result from its activation of PKA, which then phosphorylates specific effector molecules. PKA is widespread in cells, but unlike the diffusible cAMP, is largely (if not entirely) localized at discrete sites via association of its specific R subunit dimer with a specific AKAP. Proteins that contain AKAP sequences act as scaffolds for the assembly of PKA with other components to assure specificity of its action in space and time (22). PKA plus additional enzymes, substrates, and regulators constitute a molecular machine for the accurate reception, transduction, and integration of cAMP signals, with others initiated, propagated, and transmitted by chemical, electrical, or mechanical means. AKAP assemblies that coordinate cAMP effects via PKA-dependent and PKA-independent pathways include the remarkable AKAP complex in cardiac muscle where PDE4D3 acted as an adaptor for Epac, as well as a regulator of cAMP levels (23). In contrast, HEK293 cells contained PKA or Epac and PDE3B or PDE4 in different

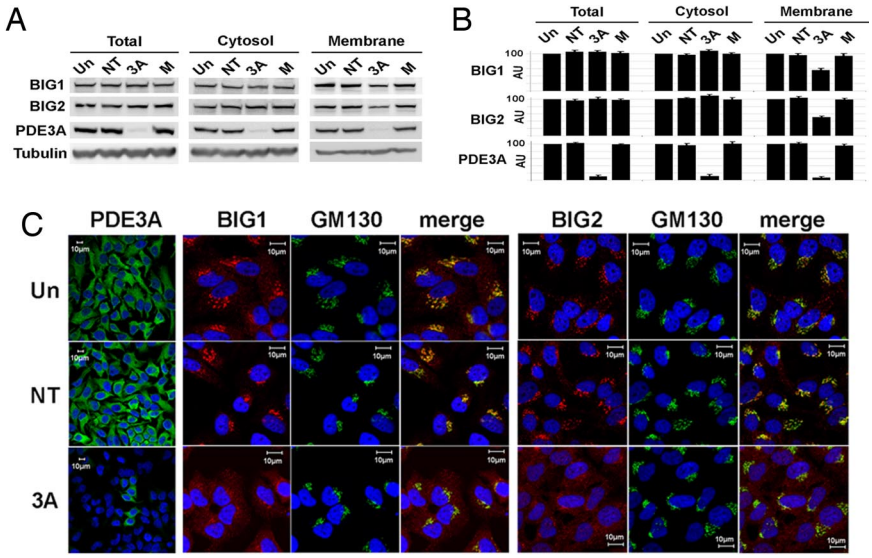

Fig. 5. Effect of PDE3A depletion with siRNA on BIG1 and BIG2 distribution in cells. (*A*) Cells untreated (Un) or transfected 48 h earlier with nontargeting (NT) or human PDE3A specific siRNA (3A) or with vehicle alone (M) were fractionated as in Fig. 4. Samples of total postnuclear fraction (1/25), cytosol (1/25), and membranes (1/6) were separated by SDS/PAGE before IB with indicated antibodies. (*B*) For each experiment, densitometric amounts of the same protein in differently treated samples were expressed relative to that of protein in untreated cells = 100. Shown are means ± 1/2 the range of values from 2 experiments like that in *A*. (*C*) Effect of PDE3A depletion with siRNA on distribution of BIG1, BIG2, and GM130 in HeLa cells. Cells were untreated or incubated 48 h with control nontargeting or specific PDE3A siRNA before inspection by using confocal immunofluorescence microscopy.

complexes, but none contained both PKA and Epac or 2 PDEs (24). Such different characteristics exemplify extensive diversities (function, size, composition, stability) among these dynamic multimolecular machines.

We initially asked whether PDE4, which had been most often reported with AKAP complexes, might interact also with BIG1 or BIG2. Known PDE4 isoforms were not detected in BIG1 and BIG2 IPs, but PDE3A was present in both along with PKA RIα. To explore functional consequences of PDE3A interaction with BIG1 and BIG2, we assessed the effects of 8-Br-cAMP on co-IP, finding that its presence doubled the amount of PDE3A recovered with IP of BIG1 or BIG2. In myocytes (22, 23), PKA-catalyzed phosphorylation of serine 13 increased PDE4D3 affinity for mAKAP, facilitating its recruitment to the complex where it hydrolyzed cAMP to restore basal levels. A similar negative feed-back mechanism could explain the reported phosphorylation of PDE3A in platelets by PKA (25), and also our observations, which still lack details of molecular interactions and phosphorylation events.

Our laboratory had found that incubation of HepG2 cells with 8-Br-cAMP resulted in partial dissociation of BIG1 and BIG2

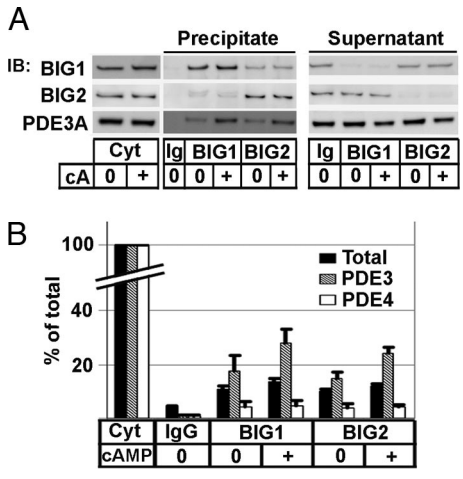

Fig. 6. Effect of cAMP on IP of PDE3A and PDE4 with BIG1 and BIG2. Cytosol (500 μL/500 μg) was incubated 30 min with 1 mM 8-Br-cAMP before IP with control IgG or antibodies against BIG1 or BIG2. (*A*) Samples of cytosol (1/25), of precipitated proteins (1/12), and IP supernatants (1/25) were analyzed as in Fig. 3C. (*B*) PDE activities of immunoprecipitated fractions are reported as in Fig. 1*B*.

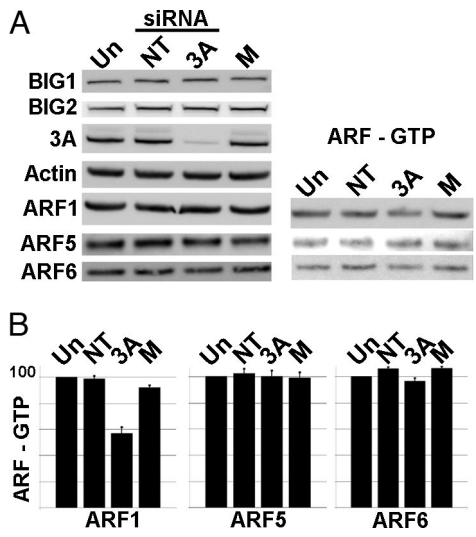

Fig. 7. Effect of PDE3A depletion on amounts of activated ARF1. (*A*) Postnuclear supernatant, (500 μL/750 μg) from cells untreated (Un) or transfected 48 h earlier with nontargeting (NT) or PDE3A siRNA (3A), or with vehicle alone (M), was incubated with immobilized GST-GGA3 to bind activated ARF-GTP. Samples of lysate (20 μg) and of GST-GGA3-bound proteins (1/6) were analyzed by Western blotting with indicated antibodies. On replicate blots, ARF-GTP bound to GST-GGA3 was identified with ARF-specific antibodies. (*B*) ARF-GTP quantified by densitometry was expressed relative to that of the same ARF-GTP in untreated cells = 100. Data are means ± SD of values from 3 experiments like that in *A*.

CELL BIOLOGY

from membranes and accumulation of BIG1 in nuclei (14). In other experiments, amounts of BIG1 and BIG2 in membrane fractions of cells incubated with okadaic acid to inhibit phosphatases were similarly decreased, without changes in nuclear fractions (15). As shown here, effective inhibition of PDE3A activity via its depletion with specific siRNA resulted in lesser amounts of BIG1 and BIG2 associated with membranes, most apparent at Golgi structures, consistent with reported effects of cAMP elevation (14, 15). It seems likely that phosphorylation of BIG1 and BIG2 by PKA was enhanced as cAMP accumulated in the vicinity when hydrolysis by PDE3A diminished. To evaluate changes in GEP activity consequent to PDE3A depletion, we used a GGA3 pull-down assay to quantify activated endogenous ARF-GTP (21, 26). PDE3A depletion did not alter total ARF1, 5, or 6, but recovery of active ARF1 was significantly lower, whereas amounts of active ARF5 (class II) and ARF6 (class III) were unchanged. These results, and previous data (8, 27), confirm a specificity of endogenous intracellular BIG1 and BIG2 for class I ARFs, despite a sometimes apparent lack of ARF specificity of GEP activity of the highly conserved Sec 7 domains from different GEPs when assayed in vitro (28).

PKA-catalyzed phosphorylation of serine 883 in BIG1, was required for nuclear accumulation of the protein in HepG2 cells incubated with 8-Br-cAMP (14). The absence of nuclear accumulation of BIG2 in those cells was not surprising, because the BIG2 molecule contains no serine corresponding to BIG1 S883. Incubation of HeLa cells with 8-Br-cAMP similarly caused BIG1 accumulation in nuclei. However, neither BIG1 nor BIG2 was seen in nuclei of HeLa cells after PDE3A depletion, presumably because elevation of cAMP in such cells occurred only in cellular microdomains in which PDE3 regulated its concentration. PKA activity at those sites is apparently not involved in 8-Br-cAMP-induced nuclear accumulation of BIG1, consistent with a role for PDE3A in restricting cAMP action in time and space to a BIG1 AKAP-defined domain. The role of an AKAP in assembling and maintaining the dynamic structures of multimolecular complexes is undoubtedly critical. It is also clear that the many AKAP proteins have diverse and specialized additional functions. Thus, we may infer the existence at different times and places in cells of a very large number of macromolecular complexes comprising constantly replaced assortments of specific proteins. The complexes function as molecular machines to receive, transduce, and propagate or transmit with precision signals initiated by chemical, electrical, or mechanical stimuli. Thus, IP of any single component must bring with it an enormous variety of different molecules no matter how seemingly ''purified'' the preparation from which it is selected.

However, we can conclude that PDE3A interacts with BIG1 and BIG2 in HeLa cell cytosol, and has a role in the regulation of vesicular trafficking via actions of BIG1 and BIG2, including their activation of ARF1. Elucidation of the molecular mechanisms involved and identification of additional components of BIG1 and BIG2 functional complexes are goals of continuing studies.

Materials and Methods

Antibodies and Other Materials. Affinity-purified antibodies against human BIG1 and BIG2 have been described (18). Polyclonal antibodies affinity-purified from rabbits immunized with human PDE3A peptides corresponding to positions 1095–1110 (29) (RLAGIENQSLDQTPQS) or 1127–1141 (GKPRGEEIPTQKPDQ) (30) of PDE3A were used, respectively, for Western blotting and IP. Rabbit polyclonal antibodies against PDE3B, mouse monoclonal antibodies against ARF1 and ARF6 were purchased from Santa Cruz, against ARF5 from Abnova, and against RIα, RIIα, RIβ, RIIβ, and C subunits of PKA, and GM 130 from BD Biosciences; rabbit polyclonal antibodies against all PDE4 forms from Abcam; HRP-conjugated goat anti-rabbit IgG and goat anti-mouse IgG from Pierce; FITC-conjugated goat anti-mouse IgG from Sigma; Alexa Fluor 594 goat and Alexa Fluor 488 goat anti-rabbit IgG from Invitrogen; protein A-Sepharose CL-4B beads from Amersham Biosciences, and 8-Br-cAMP from Sigma-Fluka.

Cell Growth, Fractionation, IP, and Western Blotting. HeLa cells (American Type Culture Collection) were grown at 37 °C, in DMEM (GIBCO) with 10% FBS (GIBCO), penicillin (100 units/mL), and streptomycin (100 μg/mL), in an atmosphere of 5% CO_2/95% air. For fractionation, cells ($\approx 20 \times 10^6$) collected by centrifugation after scraping were homogenized (20 strokes) in a Dounce tissue grinder in buffer A (100 mM NaCl/50 mM Hepes, pH 7.5/50 mM sucrose/10 mM sodium pyrophosphate/5 mM NaF/1 mM EDTA/1 mM Na_3VO_4/1 μM okadaic acid, and Roche protease inhibitor mixture). Homogenates were centrifuged (800 $\times$ *g*, 10 min), and supernatants (postnuclear fractions) were centrifuged (105,000 $\times$ *g*, 1.5 h) to separate cytosol and membrane fractions. For IP, cytosol (500 μg/500 μL) or column fractions (240 μL) containing 1% (vol/vol) Nonidet P-40, were incubated for 1.5 h with 40 μL of protein A-Sepharose CL-4B bead slurry (50% vol/vol). Beads were discarded and antibodies (5 μg) against BIG1, BIG2, or PDE 3A or control rabbit IgG were added, followed by incubation overnight (18 h) at 4 °C and addition of protein A-Sepharose CL-4B beads (50 μL) for 3 h. After centrifugation, supernatants were collected; beads were washed 3 times with buffer B (buffer A containing 250 mM sucrose), dispersed in 200 μL of buffer B, and divided into equal portions, one for elution of bound proteins in 120 μL of gel-loading buffer and separation of samples (20 μL) by SDS/PAGE in 4–12% gels, the other for assay of PDE activity. For immunoblotting (IB), proteins transferred from gels to nitrocellulose were incubated with indicated primary antibodies, followed by HRP-conjugated goat anti-rabbit or goat anti-mouse IgG secondary antibodies, and detection using SuperSignal Chemiluminescent substrate (Pierce). Immunoreactive bands were quantified by densitometry using FUJI Image Gauge V4.0 software (Fujifilm).

The cAMP PDE Assay. Total or specific PDE3 and PDE4 activities were measured as described (17), with 0.1 μM [^{3}H]cAMP [35,000 counts per minute (c.p.m.) per 300 μL of assay] as substrate.

Superose 6 Gel Filtration of HeLa Cell Cytosol. Samples of cytosol (3 mg/mL), prepared as described for IP and concentrated (Centriprep; Millipore), were applied to a column of Superose 6 HR (1 $\times$ 30 cm; Amersham) that was equilibrated and eluted with buffer A containing 150 mM NaCl and no sucrose. Samples (20 μL) of fractions (500 μL) were used for IB and assay of PDE3 activity.

Confocal Immunofluorescence Microscopy. Cells grown on 4-well CultureSlides (BD Biosciences) were washed 3 times with PBS containing 1 mM $CaCl_2$ and 1 mM $MgCl_2$ (PBSCM), and fixed (20 min) with 4% paraformaldehyde in PBSCM. After washing with PBSCM, permeabilization (4 min) with 0.1% Triton X-100 in PBSCM, washing with PBSCM, and incubation (1 h) with blocking buffer (10% goat serum in PBSCM), primary antibodies diluted in blocking buffer (BIG1 1:500; BIG2, PDE3A, 1:200; GM130 1:250) were added for 2 h. After washing with PBS, cells were incubated (1 h) with Alexa Fluor-labeled secondary antibodies diluted 1:1,000 in blocking buffer, washed with PBSCM, and mounted in Prolong Gold antifade reagent with DAPI (Invitrogen). For colocalization, antibodies against BIG1, BIG2, or PDE3A labeled with Zenon Alexa Fluor 488 (BIG1 and BIG2) or Alexa Fluor 594 (PDE3A) Rabbit IgG Labeling Kits (Invitrogen-Molecular Probes), were applied for 1 h in blocking buffer. After washing with PBSCM and mounting, cells were inspected and imaged by using confocal fluorescence microscopy (LSM 510; Zeiss).

Depletion of Endogenous PDE3A with siRNA. Small interfering RNA against human PDE3A (5′-GGAAGAAGAAGAAGAGAAA-3′) was designed and synthesized as Option A4 by Dharmacon Research. Findings with 2 additional siRNAs (5′-GAAGAUAUCCCGGUGUUUA-3′ and 5′-GAGAUUGGAUAUAGGGAUA-3′), which induced $\approx$90% depletion of PDE3A and no apparent adverse effects, confirmed those with the first siRNA. All other siRNAs and reagents were purchased from Dharmacon Research and used as before (31).

Quantification of ARF-GTP in HeLa Cells by Pull-Down with GST-GGA3. Preparation of GST fusion protein with human GGA3, an ARF-binding protein associated with Golgi membranes (32), and use of GST-GGA3 for pull-down of activated ARF-GTP at 4 °C was first described by Santy and Casanova (22). Briefly, cells ($\approx 5 \times 10^6$) collected by centrifugation after scraping, were homogenized on ice in 1 mL of 50 mM Tris, pH 7.5, 100 mM NaCl, 2 mM MgCl

2, 0.1% SDS, 0.5% sodium deoxycholate, 1% Triton X-100, 10% glycerol, and Roche protease inhibitor mixture. After centrifugation (10,000 × *g*, 10 min), supernatants were incubated (1.5 h, 4 °C) with 40 μL of CL4B Sepharose beads (50% slurry, Amersham). Beads collected by centrifugation were discarded; 0.5 mL (750-μg protein) of supernatant and of GST-GGA3 (40 μg bound to glutathione-Sepharose CL4B beads, Amersham) were incubated (4 °C) overnight, and beads were washed 3 times with lysate buffer. Samples (40 μL) of proteins eluted in 120 uL of gel-loading buffer were analyzed by Western blotting and densitometry.

ACKNOWLEDGMENTS. We thank Dr. Christian Combs and Dr. Daniela Malide (National Heart, Lung, and Blood Institute Confocal Microscopy Core Facility) for invaluable help. This work was supported by the Intramural Research Program of the National Institutes of Health National Heart, Lung, and Blood Institute.

1. Rothman JE, Wieland FT (1996) Protein sorting by transport vesicles. *Science* 272:227–234.
2. Springer S, Spang A, Schekman R (1999) A primer on vesicle budding. *Cell* 97:145–148.
3. Moss J, Vaughan M (1998) Molecules in the ARF orbit. *J Biol Chem* 273:21431–21434.
4. Achstetter T, Frazusoff A, Field C, Schekman R (1988) SEC7 Encodes an Unusual, High Molecular Weight Protein Required for Membrane Traffic from the Yeast Golgi Apparatus. *J Biol Chem* 263:11711–11717.
5. Mouratou B, et al. (2005) The domain architecture of large guanine nucleotide-exchange factors for the small GTP-binding protein ARF. *BMC Genomics* 6:20.
6. Misumi Y, et al. (1986) Novel blockade by brefeldin A of intracellular transport of secretory proteins in cultured rat hepatocytes. *J Biol Chem* 261:11398–11403.
7. Morinaga N, Tsai S-C, Moss J, Vaughan M (1996) Isolation of brefeldin A-inhibited guanine nucleotide-exchange protein for ADP-ribosylation factor (ARF)1 and ARF3 that contains Sec7-like domain. *Proc Natl Acad Sci USA* 93:12856–12860.
8. Togawa A, Morinaga N, Ogasawara M, Moss J, Vaughan M (1999) Purification and cloning of a brefeldin A-inhibited guanine nucleotide-exchange protein for ADP-ribosylation factors. *J Biol Chem* 274:12308–12315.
9. Padilla PI, et al. (2003) Interaction of FK506-binding protein 13 with brefeldin A-inhibited guanine nucleotide-exchange protein 1 (BIG1): Effects of FK506. *Proc Natl Acad Sci USA* 100:2322–2327.
10. Saeki N, Tokuo H, Ikebe M (2005) BIG1 is a binding partner of myosin IXb and regulates its Rho-GTPase activating protein activity. *J Biol Chem* 280:10128–10134.
11. Shen X, et al. (2008) Interaction of brefeldinA-inhibited guanine nucleotide exchange protein (BIG)1 and kinesin motor protein KIF21A. *Proc Natl Acad Sci USA* 105:18788–18793.
12. Xu KF, et al. (2005) Interaction of BIG2, a brefeldin A-inhibited guanine nucleotide-exchange protein, with exocyst protein Exo70. *Proc Natl Acad Sci USA* 102:2784–2789.
13. Li H, Adamik R, Pacheco-Rodriguez G, Moss J, Vaughan M (2003) Protein kinase A-anchoring (AKAP) domains in brefeldin A-inhibited guanine nucleotide-exchange protein 2 (BIG2). *Proc Natl Acad Sci USA* 100:1627–1632.
14. Citterio C, et al. (2006) Effect of protein kinase A on accumulation of brefeldin A-inhibited guanine nucleotide-exchange protein 1 (BIG1) in HepG2 cell nuclei. *Proc Natl Acad Sci USA* 103:2683–2688.
15. Kuroda F, Moss J, Vaughan M (2007) Regulation of brefeldin A-inhibited guanine nucleotide-exchange protein 1 (BIG1) and BIG2 activity via PKA and protein phosphatase 1γ. *Proc Natl Acad Sci USA* 104:3201–3206.
16. Beene DL, Scott JD (2007) A-kinase anchoring proteins take shape. *Curr Opin Cell Biol* 19:192–198.
17. Ahmad F, et al. (2007) Insulin-induced formation of macromolecular complexes involved in activation of cyclic nucleotide phosphodiesterase 3B (PDE3B) and its interaction with PKB. *Biochem J* 404:257–268.
18. Yamaji R, et al. (2000) Identification and localization of two brefeldin A-inhibited guanine nucleotide-exchange proteins for ADP-ribosylation factors in a macromolecular complex. *Proc Natl Acad Sci USA* 97:2567–2572.
19. Shinotsuka C, Waguri S, Wakasugi M, Uchiyama Y, Nakayama K (2002) Dominant-negative mutant of BIG2, an ARF-guanine nucleotide exchange factor, specifically affects membrane trafficking from the trans-Golgi network through inhibiting membrane association of AP-1 and GGA coat proteins. *Biochem Biophys Res Commun* 294:254–260.
20. Shinotsuka C, Yoshida Y, Kawamoto K, Takatsu H, Nakayama K (2002) Overexpression of an ADP-ribosylation factor-guanine nucleotide exchange factor, BIG2, uncouples brefeldin A-induced adaptor protein-1 coat dissociation and membrane tubulation. *J Biol Chem* 277:9468–9473.
21. Santy LC, Casanova JE (2001) Activation of ARF6 by ARNO stimulates epithelial cell migration through downstream activation of both Rac1 and phospholipase D. *J Cell Biol* 154:599–610.
22. McConnachie G, Langeberg LK, Scott JD (2006) AKAP signaling complexes: Getting to the heart of the matter. *Trends Mol Med* 12:317–323.
23. Dodge-Kafka KL, et al. (2005) The protein kinase A anchoring protein mAKAP coordinates two integrated cAMP effector pathways. *Nature* 437:574–578.
24. Raymond DR, Wilson LS, Carter RL, Maurice DH (2007) Numerous distinct PKA-, or EPAC-based, signaling complexes allow selective phosphodiesterase 3 and phodiesterase 4 coordination of cell adhesion. *Cell Signal* 19:2507–2518.
25. Macphee CH, Reifsnyder DH, Moore TA, Lerea KM, Beavo JA (1988) Phosphorylation results in activation of a cAMP phosphodiesterase in human platelets. *J Biol Chem* 263:10353–10358.
26. Hafner M, et al. (2006) Inhibition of cytohesins by SecinH3 leads to hepatic insulin resistance. *Nature* 444:941–944.
27. Morinaga N, Adamik R, Moss J, Vaughan M (1999) Brefeldin A inhibited activity of the sec7 domain of p200, a mammalian guanine nucleotide-exchange protein for ADP-ribosylation factors. *J Biol Chem* 274:17417–17423.
28. Pacheco-Rodriguez G, Meacci E, Vitale N, Moss J, Vaughan M (1998) Guanine nucleotide exchange on ADP-ribosylation factors catalyzed by cytohesin-1 and its Sec7 domain. *J Biol Chem* 273:26543–26548.
29. Choi YH, et al. (2001) Identification of a novel isoform of the cyclic-nucleotide phosphodiesterase PDE3A expressed in vascular smooth-muscle myocytes. *Biochem J* 353:41–50.
30. Pozuelo Rubio M, Campbell DG, Morrice NA, Mackintosh C (2005) Phosphodiesterase 3A binds to 14–3-3 proteins in response to PMA-induced phosphorylation of Ser428. *Biochem J* 392:163–172.
31. Shen X, et al. (2006) Association of brefeldin A-inhibited guanine nucleotide-exchange protein 2 (BIG2) with recycling endosomes during transferrin uptake. *Proc Natl Acad Sci USA* 103:2635–2640.
32. Dell' Angelica EC, et al. (2000) GGAs: A Family of ADP-ribosylation Factor-binding Proteins Related to Adaptors and Associated with Golgi Complex. *J Cell Biol* 149:81–93.